Relaxor ferroelectric behavior and collective modes in the π-d correlated anomalous metal λ-(BEDT-TSF)$_2$FeCl$_4$

H. Matsui, H. Tsuchiya, T. Suzuki, E. Negishi, and N. Toyota
Physics Department, Graduate School of Science, Tohoku University, Sendai 980-8578, Japan
(Received 27 January 2003; published 9 October 2003)

We have investigated the microwave response at 44.5 GHz with respect to temperature T and external magnetic field H in λ-(BEDT-TSF)$_2$FeCl$_4$ forming a quasi two-dimensional electronic system with π-d correlations. At 8.3 K [$=T_{\mathrm{MI}}$, the metal-insulator (MI) transition temperature] $<T<$70 K ($=T_{\mathrm{FM}}$), the microwave dielectric constant along the c axis, ϵ_1^c, takes positive large values amounting to 1000–2000. Furthermore, the microwave conductivity σ_1^c starts to deviate resistively from the dc conductivity σ_{dc}^c, and the difference between σ_1^c and σ_{dc}^c reaches about two orders of magnitude just above T_{MI}. The present results are consistent with the previous results at 16.3 GHz, and consequently the appearance of the anomalous metallic state is confirmed. An anomalous microwave response has also been observed in the a^* and b^* directions, and there exist large anisotropies depending sensitively on the orientations. The broad maximum of ϵ_1^c around 30 K is reminiscent not of a usual ferroelectric transition, but of relaxor ferroelectric behaviors. It is expected that dielectric domains or stripes with less metallic conductions emerge inhomogeneously in the π electronic systems. Above T_{FM}, where microwave anomalies are not present, the interplane and intraplane microwave conductivities hold anisotropies $\sigma_1^c/\sigma_1^{b^*}\approx 10^3$ and $\sigma_1^c/\sigma_1^{a^*}\approx 10$. In the antiferromagnetic insulating state, σ_1^c becomes much conductive in comparison with σ_{dc}^c. Together with low frequency data, ϵ_1^c is found to exhibit a large frequency dispersion. The microwave response is not attributed to single particle excitations, but to some collective mode excitations associated with charge degrees of freedom. The H-T phase diagram of the MI transition determined by the present microwave measurements is independent of the orientations of H, and coincides well with the phase diagram obtained by the dc magnetoresistivity and magnetization. Spin waves for the hard axis are observed as an absorption peak in the width change for the microwave magnetic field applied parallel to both H and a^*.

DOI: 10.1103/PhysRevB.68.155105 PACS number(s): 72.15.Nj, 71.30.+h

I. INTRODUCTION

Organic charge-transfer salts, which form a low-dimensional π-electronic system, are well known to exhibit a wide variety of ground states with broken symmetry[1,2] such as spin density waves (SDWs),[3] charge density waves (CDWs),[4] and superconductivity.[5] Among them, the salts based on a donor molecule of bisethylenedithiotetraselenafulvalene,[6,7] abbreviated as BEDT-TSF or simply BETS, have recently attracted much attentions due to their interesting low-temperature properties depending on the temperature, magnetic field, and pressure.[8,9] Within a class of BETS compounds, the λ-type salts composed of magnetic counter anions of $FeCl_4$ and $Fe_xGa_{1-x}Cl_4$ ($x=0-1$) have been intensively focused upon, because these are the first organic metals, where quasi-two-dimensional (Q2D) π electrons interplay with localized 3d magnetic moments through a so-called π-d interaction.

The crystal structure of λ-(BETS)$_2$FeCl$_4$, which is briefly written as $FeCl_4$ salt in this paper, is triclinic with a space group $P\bar{1}$.[10] The unit cell involves four BETS cations and two $FeCl_4^-$ anions surrounded by terminal ethylenes of BETS. A fourfold column, which consists of two crystallographically independent BETS cations, aligns along the a axis through a face-to-face coupling.[10] A side-by-side overlap extends along the c axis. The quasi-two-dimensional electronic system sandwiched by insulating $FeCl_4^-$ anion layers alternates along the b^* direction.

The temperature dependence of the dc resistivity along c, ρ_{dc}^c, shows a broad maximum around 100 K.[10,11] Such a maximum has also been observed in many BEDT-TTF compounds.[5] On the other hand, the Q2D electronic system undergoes a metal-insulator transition at $T_{\mathrm{MI}}=8.3$ K, where ρ_{dc}^c rapidly increases by at least seven orders of magnitude.[10,12,13] On the other hand, the isostructural $GaCl_4$ salt exhibits superconductivity below $T_{\mathrm{sc}}=4.8$ K, above which the dc resistivity shows highly metallic states as well.[14]

The magnetic susceptibility follows a Curie-Weiss law down to about 10 K, coming from a high spin of $S_{3d}=5/2$ localized at Fe^{3+}.[11,12] The Weiss temperature is evaluated to be $\Theta\simeq -10$ K, and hence an antiferromagnetic interaction is found to exist.[10,13] The magnetic susceptibilities for fields perpendicular and parallel to c exhibit a typical anisotropy, indicating that an antiferromagnetic long-range ordering simultaneously occurs at the MI transition.[11]

There appears a remarkable drop in the magnetic susceptibility just below T_{MI}, which reveals an emergence of localized π spins, $S_\pi=1/2$.[15] Although the localized positions have not been clarified experimentally, it is expected that the π spins may exist between BETS molecules dimerized in the column along a possessing the largest transfer integrals.[10] From recent molecular orbital calculations,[16] the π-π antiferromagnetic exchange interaction $J_{\pi\pi}$ is estimated to be much larger than the d-d and π-d exchange interactions J_{dd} and $J_{\pi d}$. Among these interactions, the π-d interaction plays

a significant role in inducing coupled antiferromagnetic ordering simultaneously in both spin systems. The insulating transition may be regarded as a new type of Mott insulator induced by the π-d interaction.

In high magnetic fields above ~ 11 T at low temperatures, the antiferromagnetic insulating (AFI) ground state transits reentrantly to a metallic state,[12] where the d spins are forced ferromagnetically. Shubnikov–de Haas oscillations have been observed above 12 T, which originate from the warped cylindrical Fermi surface.[17] The cross-sectional area is determined to be about 18% of the first Brillouin zone at 10 K, which is compared with extended Hückel tight-binding band structure calculations.[10] The effective mass is enhanced to $4.1m_0$ due to electron correlations. It is noted that a superconducting state is induced at high magnetic fields between 18 and 41 T, the direction of which is exactly parallel to the a^*-c conducting plane.[18,19] This field-induced superconducting state can be explained from the viewpoint of the Jaccarino-Peter effect,[20] well established for magnetic superconductors.[21,22]

Recently, drastic nonlinear transport phenomena have been successfully observed in current-voltage characteristics well below T_{MI}.[23] Negative resistance and switching effects were also found, which strongly depend on the temperature and magnetic field.[24,25] Such phenomena have been reported so far in insulating states of mixed-stack or segregated-stack charge transfer salts.[26,27] The negative resistance reveals that there may appear some carrier decondensation mechanism when a high electric field is applied to the AFI state.

From our previous microwave measurements employing a cavity of 16.3 GHz,[28,29] we have reported that the anomalous metallic state emerges at $T_{\mathrm{MI}}<T<70$ K $(=T_{\mathrm{FM}})$, where the microwave loss is enhanced anomalously, even though the dc resistivity indicates a highly metallic state. The real part of the complex microwave conductivity along c, σ_1^c, starts to deviate from the dc conductivity, σ_{dc}^c, below T_{FM}. Just above T_{MI}, σ_1^c is lower than σ_{dc}^c by two orders of magnitude. Consequently, the dielectric constant along c, ϵ_1^c, shows a huge increase amounting to the order of 10^3.

In order to provide further information for the anomalous metallic state and the collective modes in the AFI state, we have extensively studied the microwave response at 44.5 GHz as a function of temperature and external magnetic field. Microwave electric fields are applied to three different axes, a^*, b^*, and c, to clarify the anisotropy of the dynamic response. For the AFI state, the microwave conductivities are discussed together with low frequency data to elucidate frequency dispersions in a wide spectral range. Finally, we discuss possible origins of the anomalous metallic state by the use of other related experiments.

II. EXPERIMENTAL METHOD

Single crystals of $FeCl_4$ salt with a needle shape growing along c were prepared by an electrochemical oxidation method. Microwave excitation and detection were carried out by our homemade scalar network analyzer system available to detect the lowest power of -70 dBm with a dynamic range of 90 dB. In order to obtain a microwave response, we employed a cavity perturbation technique utilizing the TE_{011} resonant mode of a cylindrical cavity made of an oxygen free copper.[2,30,31] The resonant frequency was about 44.5 GHz and the Q value changed from $\sim 10\,000$ at room temperature to $\sim 20\,000$ at 4.2 K. Since the input power never exceeded 10 μW in the present microwave measurements, heating problems were neglected down to 0.5 K. A piece of the single crystal was mounted with a tiny amount of grease on top of a quartz rod, where either electric or magnetic field components of the microwave hold a maximum. The sample's weight ranged from 1 to 7 μg, and each sample was used for each measurement to avoid extrinsic effects such as a crack owing to thermal cycling. To check the data reproducibility, we performed microwave measurements on several samples for each configuration. The typical sample size was $0.07(a^*)\times 0.03(b^*)\times 1(c)$ mm^3, the volume V_s of which was negligibly smaller than the cavity volume V_0. The filling factor $\gamma=\gamma_0 V_s/V_0$ was of the order of 10^{-6}–10^{-5}, so that an adiabatic condition was satisfied. The mode constant γ_0 takes 2.09 for the configuration of maximum electric fields.[30]

A skin depth is given by $\delta=(2\rho_{\mathrm{dc}}/\omega\mu)^{1/2}$, where ρ_{dc}, ω, and μ denote the dc resistivity, angular frequency, and magnetic permeability, respectively. In case of $\delta>d$, where d is a sample size, microwaves penetrate throughout a sample, while in case of $\delta<d$, microwaves penetrate partially into δ from a surface. The former case is called a depolarization regime and the later a skin depth regime. For these two regimes, we have to apply different schemes to calculate complex conductivities. However, the depolarization regime is found to hold in the present measurements as described in the following sections, so that here we briefly introduce how to treat the data in this regime.

For eliminating instrumental backgrounds, the procedure must be repeated twice, first with a sample installed in a cavity as denoted by subscript "s," and second without it as "0." From a resonance curve obeying a Lorentz shape, we obtain the resonant widths (Γ_s, Γ_0) and resonant frequencies (f_s, f_0). The width change $\Delta\Gamma/2f_0=(\Gamma_s-\Gamma_0)/2f_0$ and the resonance shift $\Delta f/f_0=(f_s-f_0)/f_0$ are evaluated as functions of either T or H. A complex frequency shift is defined as

$$\frac{\Delta\omega^*}{\omega_0}=\frac{\Delta f}{f_0}-i\frac{\Delta\Gamma}{2f_0}. \tag{1}$$

A complex dielectric constant $(\epsilon^*=\epsilon_1+i\epsilon_2)$ is given by[30,32]

$$\epsilon^*=1-\frac{\Delta\omega^*/\omega_0}{\gamma+n\Delta\omega^*/\omega_0}, \tag{2}$$

where n denotes a depolarization factor. A sample with a needle shape can be approximated to be a prolate ellipsoid. A complex conductivity $(\sigma^*=\sigma_1+i\sigma_2)$ is evaluated from the following relation;

$$\epsilon^*=1+4\pi\frac{i\sigma^*}{\omega}. \tag{3}$$

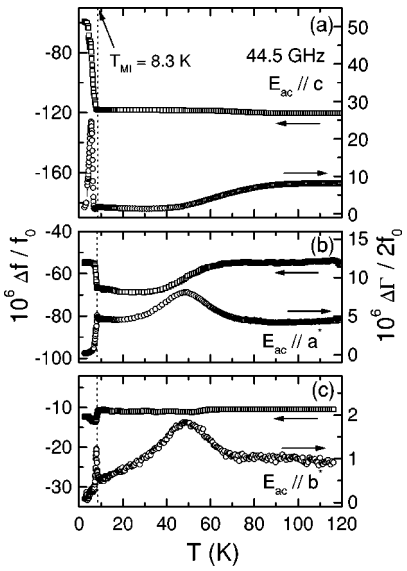

FIG. 1. Temperature dependence of the resonant shift ($\Delta f/f_0$) and width change ($\Delta\Gamma/2f_0$) at 44.5 GHz for $E_{ac}\|c$(a), $E_{ac}\|a^*$(b) and $E_{ac}\|b^*$(c).

In order to evaluate absolute values of both σ_1 and ϵ_1, it is necessary to determine a metallic shift $-\gamma/n$ precisely. The value of γ can be estimated through a measurement of the sample weight. Strictly speaking, the shape of the present sample is a slender rectangle, so that an error is involved in n obtained by assuming a prolate ellipsoid. In particular, an error of the metallic shift has a large influence on microwave conductivities for a metallic side of a depolarization regime, while in an insulating side of a depolarization regime, the error hardly gives rise to serious uncertainties of absolute values.

III. EXPERIMENTAL RESULTS

A. Temperature dependence of the microwave conductivities

The temperature dependence of $\Delta f/f_0$ and $\Delta\Gamma/2f_0$ at 44.5 GHz is depicted in Figs. 1(a)–1(c) for microwave electric field configurations of $E_{ac}\|c, a^*$, and b^*, respectively. The behaviors of $\Delta f/f_0$ and $\Delta\Gamma/2f_0$ in Fig. 1(a) are qualitatively similar to the previous results at 16.3 GHz.[28] A gradual increase of $\Delta f/f_0$ down to about 60 K reveals that the conductivity tends to rise. A maximum at around 100 K of $\Delta\Gamma/2f_0$ is in agreement with that observed in the dc resistivity. Afterwards taking the maximum, $\Delta\Gamma/2f_0$ is suppressed down to about 40 K. A shallow minimum is observed at around 30 K in $\Delta\Gamma/2f_0$. The slight increase of $\Delta\Gamma/2f_0$ at $T_{MI}<T<30$ K indicates the appearance of anomalous microwave loss. In a conventional good metal, $\Delta\Gamma/2f_0$ approaches zero with decreasing temperature.[30] An enhancement of the microwave loss was already observed at 16.3 GHz as well.[28] The dc resistivity, however, decreases monotonically by about two orders of magnitude from 100 K to T_{MI}.

According to the dc resistivity, the skin depth around 50 K is estimated to be about 30 μm, which is comparable to the sample dimension, and hence the system is expected to make a crossover from the high-temperature depolarization regime to the low-temperature skin depth regime. Nevertheless, the emergence of the anomalous microwave loss mentioned above evidences that such a crossover is not realized and that the system remains on the metallic side of a depolarization regime.

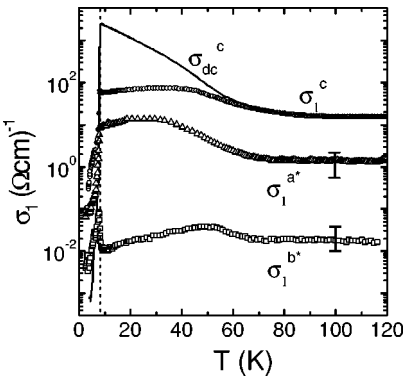

FIG. 2. Temperature dependence of the microwave conductivity σ_1 at 44.5 GHz along c, a^*, and b^* evaluated by Eqs. (2) and (3). The dc conductivity along c, σ_{dc}^c, is indicated by a solid line.

With further decreasing temperatures, drastic changes are observed in both $\Delta\Gamma/2f_0$ and $\Delta f/f_0$ at 4 K$<T<T_{MI}$, just where the resonance shape deforms from an ideal Lorentz curve, so that the data cannot help involving some errors. The sharp peak in $\Delta\Gamma/2f_0$ just below T_{MI}, which is called a depolarization peak, corresponds to a crossover from the metallic to insulating sides in a depolarization regime. Below 4 K, $\Delta f/f_0$ saturates to a nearly constant value and $\Delta\Gamma/2f_0$ decreases toward zero.

As shown in Fig. 1(b), $\Delta\Gamma/2f_0$ for $E_{ac}\|a^*$ also exhibits a depolarization peak at $\sim$50 K, around which $\Delta f/f_0$ changes most strongly. In the vicinity of the depolarization peak, the resonance shape does not deform from a Lorentz curve at all, as described above for $E_{ac}\|c$. Just below T_{MI}, a steplike change occurs both in $\Delta f/f_0$ and $\Delta\Gamma/2f_0$. A tiny peak is observed at T_{MI}, the height of which is much smaller than that of the depolarization peak around 50 K.

For $E_{ac}\|b^*$ in Fig. 1(c), $\Delta f/f_0$ is almost independent on temperature above T_{MI}. A broad peak in $\Delta\Gamma/2f_0$ around 50 K is not attributed to a depolarization peak, because $\Delta f/f_0$ hardly varies at the peak temperature. Below T_{MI}, $\Delta f/f_0$ shows a steplike change and $\Delta\Gamma/2f_0$ is suppressed toward zero after taking a tiny peak just below T_{MI}.

Figure 2 depicts the microwave conductivities for each orientation evaluated by Eqs. (2) and (3) in a depolarization regime. Filling factors of the samples are estimated to be $\gamma = 2.7\times10^{-6}$, 1.1×10^{-5}, and 7×10^{-6} for c, a^*, and b^*, respectively. The dc resistivity only along c, ρ_{dc}^c, has been measured so far. The temperature dependence of σ_{dc}^c ($\equiv 1/\rho_{dc}^c$) is shown by a solid line in Fig. 2. The metallic increase occurs down to T_{MI}, and the rapid decrease reaches about seven orders of magnitude from T_{MI} to 4.2 K.

We have already described that the anomalous microwave loss emerges in $E_{ac}\|c$ at $T_{MI}<T<40$ K, whereas the microwave response never shows any anomalies at higher temperatures. In order to determine the depolarization factor

along c, n_c, we assume that σ_1^c is equal to σ_{dc}^c at $T=100$–150 K. Then we obtain $n_c=2.27\times10^{-2}$, which is larger than 1.2×10^{-2} estimated by assuming a prolate ellipsoid. Above 60 K, σ_1^c coincides with σ_{dc}^c, and, at lower temperatures, σ_1^c becomes much resistive in comparison to σ_{dc}^c, and a shallow maximum appears around 30 K in accordance with a minimum of $\Delta\Gamma/2f_0$ [Fig. 1(b)]. Just above T_{MI}, the difference between σ_1^c and σ_{dc}^c amounts to about two orders of magnitude. The resistive feature in σ_1^c is consistent with the previous results at 16.3 GHz.[28]

For a depolarization peak, we can apply a relation of[30]

$$\Delta f/f_0+\gamma/n=\Delta\Gamma/2f_0. \tag{4}$$

At the depolarization peak along a^* in Fig. 1(b), $\Delta\Gamma/2f_0$ takes 8.3×10^{-6}, which corresponds to the left hand side of Eq. (4) representing the relative difference. There are no data on the dc conductivity along a^*, so that we employ the depolarization factor of $n_{a^*}=0.14$ calculated through an assumption of a prolate ellipsoid, and $\sigma_1^{a^*}$ is estimated to be 1 $(\Omega\,\mathrm{cm})^{-1}$ around 100 K. The error in n_{a^*} ranges from 0.1 to 0.4 at most, and hence $\sigma_1^{a^*}$ are evaluated to be around 0.5–2 $(\Omega\,\mathrm{cm})^{-1}$ around 100 K, as indicated by an error bar in Fig. 2. Below 70 K, $\sigma_1^{a^*}$ gradually increases and exhibits a shallow maximum around 30 K, which is close to the maximum temperature in σ_1^c.

To calculate $\sigma_1^{b^*}$, the depolarization factor is estimated to be $n_{b^*}=0.72$ through the calculation for a prolate ellipsoid. The absolute value of $\sigma_1^{b^*}$ does not depend much on either n_{b^*} or the metallic shift, because the whole temperature range belongs to an insulating side of a depolarization regime. We estimate the error of the absolute value to be $4\times10^{-2}\sim1\times10^{-2}$ around 100 K, as denoted by an error bar. As shown in Fig. 2, $\sigma_1^{b^*}$ is almost constant, though it takes a maximum around 50 K.

Below T_{MI}, σ_1^c exhibits a sudden drop by about three orders, whereas it is more conductive than σ_{dc}^c suppressed to the order of 10^{-4} $(\Omega\,\mathrm{cm})^{-1}$. A similar suppression is also observed in $\sigma_1^{a^*}$, the magnitude of which is approximated to be two orders. Just below T_{MI}, $\sigma_1^{b^*}$ shows a remarkable peak corresponding to the peak observed in $\Delta\Gamma/2f_0$ in Fig. 1(c). The variations of $\sigma_1^{b^*}$ below and above T_{MI} are much smaller than those of σ_1^c and $\sigma_1^{a^*}$.

At high temperatures above T_{FM}, the intraplane σ_1^c is approximated to be 10^3 times as large as the interplane conductivity $\sigma_1^{b^*}$. A large discrepancy is similarly found in the ratio of 10^3–10^5 between intraplane and interplane dc conductivities as reported in α-$(BEDT\text{-}TTF)_2KHg(SCN)_4$ (Refs. 5 and 33) and α-$(BEDT\text{-}TTF)_2TlHg(SeCN)_4$.[34] On the other hand, $\sigma_1^{a^*}$ is approximately one order less conductive than σ_1^c. Thus the two-dimensional conduction on the a^*-c plane is concluded to be highly anisotropic. Here we make some comments on the intraplane anisotropy. Little intraplane anisotropy has so far been reported for κ-type salts such as κ-$(BEDT\text{-}TTF)_2Cu(NCS)_2$,[35] though the aforementioned α-type BEDT-TTF salts hold anisotropies of similar magnitudes to the present $FeCl_4$ salt at room temperature.[5,33,34] Both α- and λ-type salts take columnar structures, and different conductions are obtained for directions parallel or perpendicular to the column. Generally speaking, conductions along the column are simply expected to be the largest. In $FeCl_4$ salt, however, the most conductive direction is not a, along the columnar direction, but c, along the intercolumnar direction, which is consistent with band structure calculations.[10]

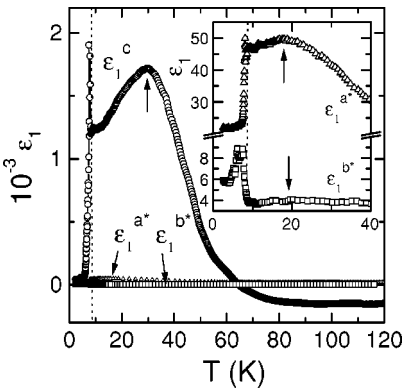

FIG. 3. Temperature dependence of dielectric constants at 44.5 GHz obtained by Eq. (2) along c, a^*, and b^*. In the inset, $\epsilon_1^{a^*}$ and $\epsilon_1^{b^*}$ are enlarged below 40 K.

The temperature dependence of the dielectric constants, which are calculated with Eq. (2), is shown in Fig. 3. The sign of ϵ_1^c changes from negative to positive around T_{FM}. The metallic state above T_{FM} is considered to have no anomalies. However, ϵ_1^c takes extremely large positive values in quite anomalous metallic states at $T_{MI}<T<T_{FM}$, where σ_1^c becomes dispersive as mentioned above. A broad maximum in ϵ_1^c is seen around 30 K, which amounts to 1700 ± 500. The error comes from the uncertainty of n_c. Afterward taking a sharp peak at T_{MI}, ϵ_1^c drops drastically and saturates to 45 ± 15 below 5 K.

Both $\epsilon_1^{a^*}$ and $\epsilon_1^{b^*}$ show slight increases below T_{FM}, which exhibit a broad maximum around 20 K as shown in the inset of Fig. 3. These increases indicate that the anomalous microwave response develops as well as in ϵ_1^c at $T_{MI}<T<T_{FM}$. The values of $\epsilon_1^{a^*}$ and $\epsilon_1^{b^*}$ are 2–3 orders of magnitude smaller than that of ϵ_1^c. Reflecting highly anisotropic conductivities in Fig. 2, the dielectric constants also reveal anisotropies depending on the orientations. Afterwards taking sharp peaks, $\epsilon_1^{a^*}$ and $\epsilon_1^{b^*}$ saturate well below T_{MI} to 22 ± 5 and 6 ± 1, respectively.

B. Magnetic field dependence of the microwave conductivities for $E_{ac}\|c$

Figure 4 shows the resonant shift (a) and width change (b) for the configuration of $E_{ac}\|c$ versus T under $H=0\sim12$ T applied parallel to a^*. At higher fields than $H_c\sim11$ T, the critical fields for the reentrant transition, $\Delta f/f_0$ and $\Delta\Gamma/2f_0$ remain almost constant down to 0.6 K. The MI transition

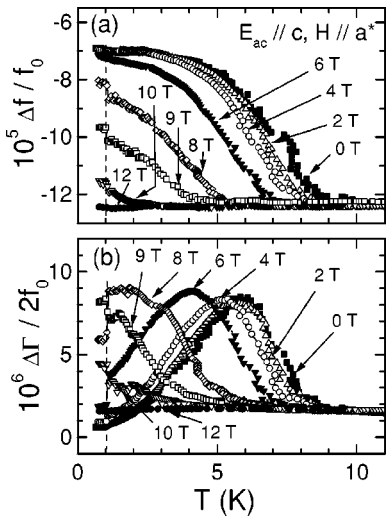

FIG. 4. Temperature dependence of $\Delta f/f_0$ (a) and $\Delta\Gamma/2f_0$ (b) for $E_{ac}\|c$ at different external magnetic fields applied parallel to a^*.

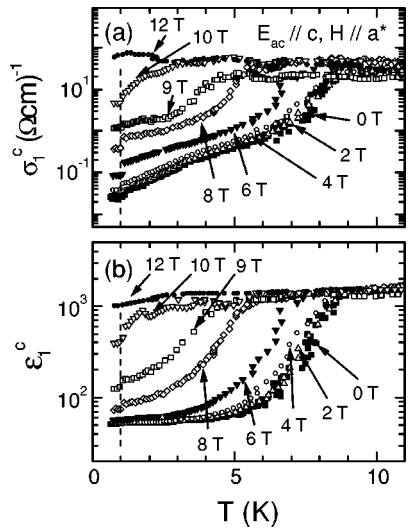

FIG. 6. Temperature dependence of σ_1^c (a) and ϵ_1^c (b) at different external magnetic fields applied parallel to a^*.

temperatures are defined by assuming that $\Delta f/f_0$ and $\Delta\Gamma/2f_0$ start to deviate from the constant values. With increasing H, a remarkable increase of $\Delta f/f_0$ in the AFI states is suppressed and vanishes at 12 T. On the other hand, the depolarization peak in $\Delta\Gamma/2f_0$ shifts to lower temperatures. It must be noted again that uncertainties become large in the temperature range around the depolarization peak owing to deviations of the resonance shape from a Lorentz curve. A discrete jump takes place around 1 K in the AFI state, which is observed up to 10 T.

The results of the configurations for $E_{ac}\|c$ and $H\|b^*$ are depicted in Fig. 5. The steplike increase of $\Delta f/f_0$ is reduced by H, and the depolarization peak of $\Delta\Gamma/2f_0$ shifts to lower temperatures due to a suppression of T_{MI}. The temperature dependence in Fig. 5 is qualitatively similar to that in Fig. 4.

The real part of the complex conductivity and dielectric constant, which are evaluated by Eqs. (2) and (3) with the data in Figs. 4 and 5, are shown in Fig. 6 for $H\|a^*$ and in Fig. 7 for $H\|b^*$. In the delocalized π electronic states, σ_1^c takes a nearly constant value around 40 $(\Omega\,\mathrm{cm})^{-1}$. From Figs. 6(b) and 7(b), it is found that ϵ_1^c varies from the order 10 to 10^3 with increasing H, and consequently the large dielectric constant in the anomalous metallic state above T_{MI} is recovered below T_{MI} under higher magnetic fields than H_c. In the anomalous metallic state, the ϵ_1^c of about 1500 is almost independent of both T and H. The MI transitions in H is independent of the magnetic field directions. It is concluded that magnetic fields control the dielectric and magnetic properties in the AFI state. In Fig. 6, there are discrete jumps at 1 K in both ϵ_1^c and σ_1^c. The dc resistivity below T_{MI} rapidly increases, associated with many successive jumps accompanying a hysteresis, suggesting a first-order transition.[13,29] The resistive jumps imply that the AFI transitions may be accom-

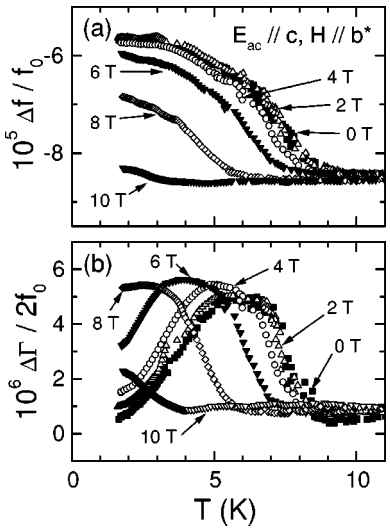

FIG. 5. Temperature dependence of $\Delta f/f_0$ (a) and $\Delta\Gamma/2f_0$ (b) for $E_{ac}\|c$ at different external magnetic fields applied parallel to b^*.

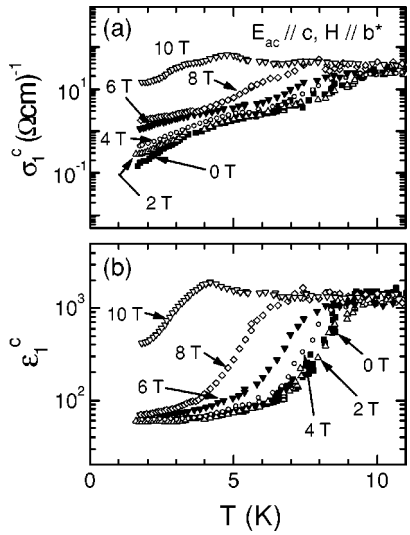

FIG. 7. Temperature dependence of σ_1^c (a) and ϵ_1^c (b) at different external magnetic fields applied parallel to b^*.

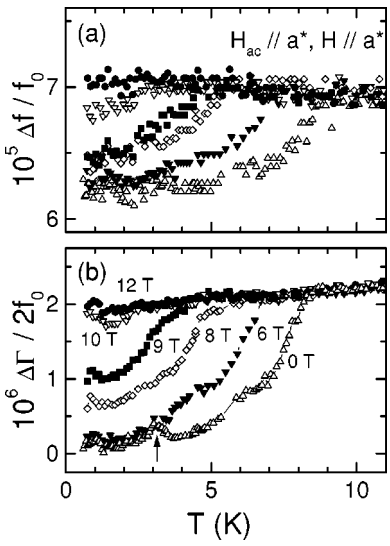

FIG. 8. Temperature dependence of $\Delta f/f_0$ (a) and $\Delta\Gamma/2f_0$ (b) for $H_{ac}\|a^*$ at different external magnetic fields applied parallel to a^*.

panied by many metastable states. It is unclear, however, whether the jumps at 1 K in ϵ_1^c and σ_1^c relate to the metastable states or not.

C. Magnetic field dependence of the microwave conductivities for $H_{ac}\|a^*$

In Fig. 8, a microwave magnetic field H_{ac} is applied parallel to a^*, and hence an eddy current should be induced in the b^*-c plane. Since the least conducting direction is b^* as shown in Fig. 2, an eddy current is expected to be so negligible that the dominant contribution comes from a complex magnetic susceptibility due to the π and d spins. Both $\Delta f/f_0$ and $\Delta\Gamma/2f_0$ at 0 T are rapidly suppressed below T_{MI}. With increasing H applied parallel to a^*, the MI transition temperatures decrease. The insulating state disappears at 12 T, and $\Delta f/f_0$ and $\Delta\Gamma/2f_0$ take nearly constant values without depending on magnetic fields.

In the zero field data an anomalous peak, where the microwave absorption increases, is observed in $\Delta\Gamma/2f_0$ around 3 K, while the peak disappears above 6 T. As shown in Fig. 9, the peak temperature and the height depend on H in a complicated way. The behaviors are quite different below and above 1.2 T. To note, the microwave absorptions become so large at 4.1 T$<H<$5 T that the resonance shape deforms from a Lorentz curve, and hence we display only the data below 4.1 T. At $0 \leqslant H < 1.2$ T, the absorption peak shifts to higher temperatures and the height becomes gradually small. At 2 T, the peak temperature becomes highest. The height tends to increase in the low temperature range, though the peak becomes suddenly broadened around 3.5 T. Since no peak has been observed for the response to E_{ac} in Figs. 4 and 5, the peaks observed in H_{ac} are attributed to a dynamic response due to spin degrees of freedom.

IV. DISCUSSION

First of all, we discuss the dynamic response in the AFI state, together with low frequency dielectric constants obtained so far. As displayed in Fig. 2, σ_1^c below T_{MI} is found to be reduced by three orders of magnitude, which is much more conductive than σ_{dc}^c. Similar conductive features for the high frequency response have been reported for various ground states such as SDWs, CDWs, and charge disproportionation (CD) in organic conductors.

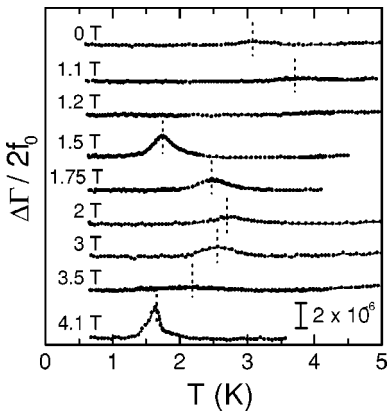

FIG. 9. Temperature dependence of $\Delta\Gamma/2f_0$ for the configuration of $H_{ac}\|H\|a^*$ below 4.1 T. The peak fields are indicated by dotted lines.

In case of quasi one-dimensional conductor $(TMTSF)_2PF_6$, σ_1^a in a microwave frequency range is suppressed only one order of magnitude below the SDW transition temperature of $T_{SDW}=12$ K.[36,37] For the drastic frequency dispersion of σ_1^a, collective excitations have been identified due to the internal deformations in a radio frequency range and the phason at $q=0$ around 0.1 cm^{-1}. The dielectric constant ϵ_1^a also exhibits a large dispersion; 10^9 at kHz-range frequencies to 10^5 at microwave frequencies. In α-$(BEDT\text{-}TTF)_2I_3$, the insulating ground state below 135 K was recently found to be associated with CD by ^{13}C-NMR measurements.[38] The microwave conductivities at 10–600 GHz are much higher than the dc conductivity and include the large dispersion.[39] Variations of the dielectric constants amount to the order of 10^3 at 100 Hz–100 GHz.

Below T_{MI}, we have already measured the dielectric constants at low frequencies from 12.3 Hz to 104 kHz by a three-terminal method utilizing a capacitance bridge.[40] Figure 10 depicts the temperature dependence of ϵ_1^c below T_{MI}, together with ϵ_1^c at 16.3 and 44.5 GHz. In this low frequency

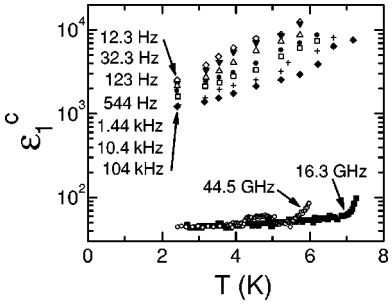

FIG. 10. Dispersion of ϵ_1^c in the AFI state at frequencies between 12.3 Hz and 44.5 GHz.

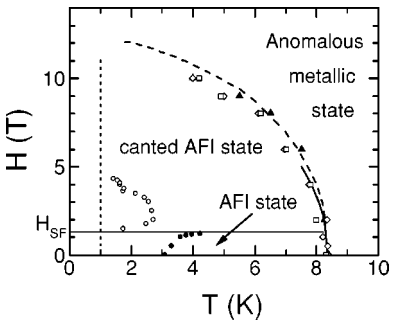

FIG. 11. *H-T* phase diagram in the AFI state determined from the configurations of $E_{ac}\|c$ and $H\|a^*$ (closed triangles), $E_{ac}\|c$ and $H\|b^*$ (open squares), and $H_{ac}\|a^*$ and $H\|a^*$ (open diamonds). The broken and solid curves are obtained from the dc resistivity and magnetization. The *H-T* dependence of the peaks in Fig. 9 is shown by closed circle in the AFI state below H_{SF} and open circles in the canted AFI state above H_{SF}. The dotted vertical line is determined by the jumps at 1 K in Figs. 4 and 6.

range, ϵ_1^c amounts to the order of 10^3–10^4, which is systematically dispersive with frequency. For both 16.3 and 44.5 GHz, ϵ_1^c almost saturates to be about 45. Although ϵ_1^c in a radio frequency range has not yet been measured, it is certain that there exists an extremely large dispersion in ϵ_1^c.

The π electrons are localized below T_{MI}, whereas the present results obtained in σ_1^c and ϵ_1^c indicate that the π electrons exhibit a highly conducting response to microwave electric fields under high frequencies. From the temperature dependence of ρ_{dc}^c, a charge gap due to the localization of π electrons is evaluated to be $2\Delta_{MI}=14\ (\pm 2)$ K.[23] The microwave energy is one order of magnitude lower than $2\Delta_{MI}$, and consequently single particle excitations are negligible even if they exist. The present response could be attributed to some unknown collective modes due to charge degrees of freedom in the localized π electrons. According to the theoretical calculations, the transfer integrals along *a* are described by t_A, t_B, t_{A^*} ($\simeq t_A$), and t_C for four BETS molecules in the unit cell. Among these, the largest t_A and t_{A^*} generate a dimer character.[41] Consequently π electrons tend to localize in the intramolecular sites A and A*, and charge orderings might be induced in the conducting *a-c* plane. The observed collective modes correspond to the dynamics of this charge ordering.

Figure 11 shows the *H-T* phase diagram for the MI transition determined by the present microwave data in addition to the results of the dc magnetoresistivity and magnetization obtained so far by our group.[13] The microwave data measured in different configurations coincide well not only with each other, but also the results of the dc magnetoresistivity and magnetization. The detail of the diagram will be published elsewhere.[42]

The absorption peaks in Fig. 9 are plotted by open and closed circles in Fig. 11. The configuration of $H_{ac}\|H\|a^*$ corresponds not to a usual electron spin resonance (ESR), but to a parallel pumping to measure $k\neq 0$ spin waves. From recent ESR measurements,[43,44] the spin waves have been detected as an antiferromagnetic resonance (AFMR) below T_{MI} at frequencies from 23 to 110 GHz. The frequency-field profile is basically explained by a two-sublattice model with a biaxial magnetic anisotropy. The spin wave is considered to be excited in the localized π spin system due to extremely large $J_{\pi\pi}=448$ K.[16] The AFMR measurements confirm that the easy axis is parallel to the direction tilted by about 30° from *c* to *b**, which has been pointed out by the torque experiments.[45,46] The intermediate axis is perpendicular to the easy axis in the *b*-c* plane, and the hard axis is close to *a**. The spin-flip field is confirmed to be $H_{SF}=1.3$ T by the frequency-field profile. The *H-T* dependence below H_{SF}, denoted by closed circles in Fig. 11, is in good agreement with the temperature dependence of the AFMR for $k=0$ spin waves along the hard axis. In the canted AFI state above H_{SF}, the *H-T* dependence denoted by open circles was not found in AFMR studies.[43,44] The absorption above H_{SF} is attributed to $k\neq 0$ spin waves. A vertical dotted line at 1 K is determined by the jumps observed in Figs. 4 and 6. Since there is no anomaly at 1 K for the H_{ac} configuration, as shown in Fig. 8, the jumps for the E_{ac} configuration correspond to the charge degrees of freedom in localized π electrons.

As shown in Fig. 3, there appears a sharp peak in ϵ_1^c at T_{MI}. The low-frequency ϵ_1^c in Fig. 10 tends to increase divergently towards T_{MI}, suggesting a peak at T_{MI}. In fact, it is quite difficult to measure ϵ_1^c approaching T_{MI}, because of the drastic increase of the conductivity component. At T_{MI}, ρ_{dc}^c increases by about seven orders of magnitude together with a temperature hysteresis.[12,13] A noticeable jump of the magnetic susceptibility also exhibits a hysteresis around T_{MI}.[13] Furthermore, recent x-ray diffraction experiments have revealed that the lattice constants exhibit a discontinuous jump at T_{MI},[47] providing evidence of a first-order structural phase transition. Although a structural analysis has not yet been made, a possible structural phase transition should reduce the symmetry from $P\bar{1}$ to $P1$ uniquely. If this scenario is true, the MI transition may accompany a ferroelectric transition as well as an antiferromagnetic transition spontaneously.

Finally, we discuss the anomalous metallic state that emerges at $T_{MI}<T<T_{FM}$, where a huge dielectric constant is observed along *c*, accompanying anomalies of the microwave conductivities as well. An analysis on the basis of Eqs. (2) and (3) satisfies a Kramers-Kronig relation for a metal, and then the suppression of σ_1^c relates to an enhancement of ϵ_1^c due to causality.[2] In this temperature range, the magnetic susceptibility follows a Curie-Weiss law and ρ_{dc}^c shows no anomalies within an experimental accuracy. On the other hand, noticeable anomalies have been observed at T_{FM} in the specific heat[48] and ^{1}H nuclear magnetic resonance(^{1}H-NMR).[49,50] The specific heat exhibits a discrete jump with an extremely large magnitude, suggesting some structural anomalies. Above T_{FM}, a single peak exists in the ^{1}H-NMR spectrum due to the hyperfine field between the proton nuclei and π electrons. At T_{FM}, there appear two different peaks for both sides of the main peak. With decreasing temperatures, the intensities of both side peaks become large. Since the main peak still remains even below T_{FM}, the electronic state in the high temperature range above

T_{FM} coexists with the low-temperature phase that emerges below T_{FM}.

Some charge transfer salts such as α-(BEDT-TTF)$_2$I$_3$ and (TMTTF)$_2$PF$_6$ bring about CD, in which the ^{13}C-NMR shows a spectral splitting.[38,51] The splitting comes from the appearance of two differently charged sites of donor molecules. In (TMTTF)$_2$PF$_6$,[52] the dielectric constant takes a peak around 70 K, which becomes broad and shifts to higher temperature with increasing frequency. These behaviors are quite different from a usual ferroelectric transition, because the transition temperature corresponding to a sharp peak never changes by a frequency. The CD occurs in a whole region of a crystal due to a long-range Coulomb interaction, and the dc electrical resistivity shows semiconducting or insulating behaviors. Thus CD should be incompatible with a highly metallic state as in the present system. In $FeCl_4$ salt, ρ_{dc}^c exhibits a metallic decrease at $T_{MI}<T<100$ K, so that it is difficult to assume CD developed in the whole region of sample. As mentioned previously, the dimer character is significant to the Q2D electrons,[41] and thus this system may exhibit an intrinsic instability against forming CD even above T_{MI}.

It is empirically known that ρ_{dc}^c in $FeCl_4$ salt is several times as large as that in isostructural $GaCl_4$ salt below about T_{FM}.[53] This discrepancy may be related to an emergence of the anomalous metallic state in $FeCl_4$ salt. From σ_{dc}^c at low temperatures, the plasma frequency ω_{pl} is estimated to be about 10^{15} Hz, which is much larger than the present microwave frequency. According to a Drude-Sommerfeld theory for a metal,[54] conduction electrons instantaneously shield a dielectric polarization, if it emerges, and a positive dielectric constant is never induced at lower frequencies than ω_{pl}. We believe that the present π electronic system may self-decompose into two different states below T_{FM}; one maintains the metallic conduction, and the other maintains dielectric anomalies with a less metallic region. This phase separation may manifest as a domain or stripe. The aforementioned character of CD probably plays a significant role in leading domain or stripe structures. To note, no anomaly has been found in the metallic state of $GaCl_4$ salt,[28] so that the π-d interaction in $FeCl_4$ salt must make some essential contributions to the anomalous metallic state. The interaction between localized d spins and π conduction electrons can be regarded as a Ruderman-Kittel-Kasuya-Yoshida (RKKY) interaction.[55] It is quite interesting to investigate the roles of a RKKY-type π-d interaction to the dielectric anomalies in the anomalous metallic state, though further experiments are necessary to solve this novel issue.

Anomalies of the microwave conductivity have been reported for metallic states of various highly correlated electronic systems.[56] In heavy fermion compounds such as $CeAl_3$ (Ref. 57) and UPt_3,[58] σ_1 exhibits a large frequency dispersion centered at $\omega=0$ due to Kondo lattice formation. The temperature dependence of the microwave resistivity σ_1^{-1} starts to deviate from the dc resistivity proportional to T^2 at low temperatures. In CeNiSn, known as a Kondo semiconductor,[59] σ_2 exhibits an anomalous increase and σ_1 becomes lower than the dc conductivity below 10 K. The anomalies are explained by a model in which the scattering rate of the quasiparticles is rapidly reduced by the gap formation. These microwave anomalies observed in the metallic states of heavy fermion compounds are caused by low-temperature coherent electronic states extending throughout the crystals.

The enhancement of ϵ_1^c in Fig. 3 takes place in a wide temperature range in contrast to a sharp peak observed in a usual ferroelectric transition. In $SrTiO_3$,[60] a broad enhancement of ϵ_1 continues down to 4 K, which is caused by a ferroelectric fluctuation. A ferroelectric transition does not take place, but the paraelectric state is stabilized due to quantum mechanical effects. In the quantum paraelectric state, ϵ_1 amounts to about 20 000 without a temperature dependence below 4 K. Quantum paraelectrics, however, occurs in a whole region of insulating crystals, so that it is also difficult to realize in $FeCl_4$ salt.

The broad maximum of ϵ_1^c in Fig. 3 is quite reminiscent of a relaxor ferroelectric behavior,[61] which is characterized by an extremely high and dispersive maximum of dielectric constants. Relaxor ferroelectrics was observed in $Pb(Mg_{1/3}Nb_{2/3})O_3$ and related materials,[62] the dielectric constant of which reaches the order of 10^4. Several insulating organic systems were recently found to exhibit a relaxor ferroelectric behavior, for instance, in tetrathiafulvalene-*p*-chloranil salt with dopant trichloro-*p*-benzoquinone[63] and poly(vinylidene fluoride-trifluoroethylene) copolymer after electron irradiation.[64] Although many theoretical models have been presented, the origin of relaxor ferroelectrics is still controversial.

Crystal structures of relaxor ferroelectric systems hardly change in general, whereas the local symmetry in polar micro-regions or nanoregions varies from the original symmetry in an overwhelming region. Recent x-ray diffraction experiments on a single crystal of $FeCl_4$ salt observed anomalies of the lattice constant along c at T_{FM},[65] while it is not clear at present whether the lattice anomaly is caused by uniform structural transition or not. Moreover, the peak profile of the (007) Bragg reflection becomes deformed at $T_{MI}<T<T_{FM}$.[65] These facts experimentally indicate that dielectric domains or stripes emerge inhomogeneously in the π electronic systems of the crystal. The present inhomogeneous states at $T_{MI}<T<T_{FM}$ might be similar to a metal-dielectric composite with a percolation threshold of conductivity. Although the origin of the inhomogeneity has not been clarified, the anomalous metallic state should play a significant role as a precursor to a transition to a ferroelectric state interconnected to the antiferromagnetic and charge orderings below T_{MI}.

V. CONCLUSION

We have presented our microwave results at 44.5 GHz for both the anomalous metallic state and the AFI state in λ-(BETS)$_2$FeCl$_4$. Above T_{FM}, there are no anomalies in the microwave response, while the microwave conductivities are found to be highly anisotropic due to the configurations of E_{ac}. At $T_{MI}<T<T_{FM}$, the emergence of an anomalous metallic state, confirmed in the present study, was first observed in the previous microwave measurements at 16.3 GHz. A

remarkable response appears along c; ϵ_1^c is enhanced to the order of 10^3, and σ_1^c becomes resistive in contrast to σ_{dc}^c. Both the dielectric and conductive anomalies indicate large anisotropies depending on the orientations of E_{ac}. The broad peak around 30 K is reminiscent of relaxor ferroelectric behaviors. The origin of the anomalous metallic state is unsolved at present; however, the huge dielectric constant may be attributed to the formation of dielectric domains or stripes with less metallic conduction in the π electronic systems. The anomalous metallic state is an extremely unique phase in that the dielectric, magnetic, and conducting properties of π and d electrons interplay with each other. In order to clarify the origin of the anomalous metallic state, it is desired, in particular, to study the frequency dispersion of the microwave conductivities in a wide spectral range and to make a further structural analysis by x-ray diffraction experiments.

Below T_{MI}, the microwave conductivity for $E_{ac} \| c$ is very conductive in comparison with the dc conductivity, and the dielectric constants exhibit a large frequency dispersion, which varies from 45 at microwave frequencies to 10^4 at low frequencies. The dynamic response is attributed to collective modes associated with charge degrees of freedom. From the temperature dependence of σ_1^c and ϵ_1^c under H applied along a^* and b^*, the H-T phase diagram of the AFI state is determined, and it is independent of the field directions and coincides well with the phase diagram obtained by the dc magnetoresistivity and magnetization. The magnetic field dependence of the width change for $H_{ac} \| H \| a^*$ shows an anomalous peak, which originates from spin waves excited on localized π spins.

ACKNOWLEDGMENT

This work was supported by a Grant-in-Aid for Scientific Research from the Ministry of Education, Culture, Sports, Science and Technology (No. 09440141), a Grant-in-Aid from the Japan Society for the Promotion of Science (Nos. 11740182 and 13640345), and REIMEI Research Resources of JAERI. We greatly appreciate helpful discussions with Y. Noda, M. Watanabe, H. Kobayashi, T. Enoki, and T. Sasaki.

[1] G. Grüner, *Density Waves in Solids* (Addison-Wesley, Reading, MA, 1994).
[2] M. Dressel and G. Grüner, *Electrodynamics of Solids* (Cambridge University Press, Cambridge, 2002).
[3] G. Grüner, Rev. Mod. Phys. **66**, 1 (1994).
[4] G. Grüner, Rev. Mod. Phys. **60**, 1129 (1988).
[5] T. Ishiguro, K. Yamaji, and G. Saito, *Organic Superconductors* (Springer, Berlin, 1998).
[6] R. Kato, H. Kobayashi, and A. Kobayashi, Synth. Met. **41-43**, 2093 (1991).
[7] R. R. Schumaker, V. Y. Lee, and E. M. Engler, IBM Research Report, 1983.
[8] H. Kobayashi, A. Kobayashi, and P. Cassoux, Royal Soc. Chem. **29**, 325 (2000).
[9] H. Kobayashi, A. Sato, H. Tanaka, A. Kobayashi, and P. Cassoux, Coord. Chem. Rev. **190-192**, 921 (1999).
[10] H. Kobayashi, H. Tomita, T. Naito, A. Kobayashi, F. Sakai, T. Watanabe, and P. Cassoux, J. Am. Chem. Soc. **118**, 368 (1996).
[11] H. Akutsu, K. Kato, E. Ojima, H. Kobayashi, H. Tanaka, A. Kobayashi, and P. Cassoux, Phys. Rev. B **58**, 9294 (1998).
[12] L. Brossard, R. Clerac, C. Coulon, M. Tokumoto, T. Ziman, D.K. Petrov, V.N. Laukhin, M.J. Naughton, A. Audouard, F. Goze, A. Kobayashi, H. Kobayashi, and P. Cassoux, Eur. Phys. J. B **1**, 439 (1998).
[13] H. Uozaki, Ph.D. thesis, Tohoku University, 2001.
[14] H. Kobayashi, T. Udagawa, H. Tomita, K. Bun, T. Naito, and A. Kobayashi, Chem. Lett. **1993**, 1559.
[15] M. Tokumoto, T. Naito, H. Kobayashi, A. Kobayashi, V.N. Laukhin, L. Brossard, and P. Cassoux, Synth. Met. **86**, 2161 (1997).
[16] T. Mori and M. Katsuhara, J. Phys. Soc. Jpn. **71**, 826 (2002).
[17] S. Uji, H. Shinagawa, C. Terakura, T. Terashima, T. Yakabe, Y. Terai, M. Tokumoto, A. Kobayashi, H. Tanaka, and H. Kobayashi, Phys. Rev. B **64**, 024531 (2001).
[18] S. Uji, H. Shinagawa, T. Terashima, T. Yakabe, Y. Terai, M. Tokumoto, A. Kobayashi, H. Tanaka, and H. Kobayashi, Nature (London) **410**, 908 (2001).
[19] L. Balicas, J.S. Brooks, K. Storr, S. Uji, M. Tokumoto, H. Tanaka, H. Kobayashi, A. Kobayashi, V. Barzykin, and L.P. Gorkov, Phys. Rev. Lett. **87**, 067002 (2001).
[20] V. Jaccarino and M. Peter, Phys. Rev. Lett. **9**, 290 (1962).
[21] H.W. Muel, C. Rossel, M. Decroux, ϕ. Fischer, G. Remenyi, and A. Braggs, Phys. Rev. Lett. **53**, 497 (1984).
[22] M. Isino, K. Tsunokuni, H. Iwasaki, and Y. Muto, J. Magn. Magn. Mater. **31**, 519 (1983).
[23] N. Toyota, Y. Abe, H. Matsui, E. Negishi, Y. Ishizaki, H. Tsuchiya, H. Uozaki, and S. Endo, Phys. Rev. B **66**, 033201 (2002).
[24] Y. Abe, T. Kuwabara, H. Tsuchiya, Y. Ishizaki, E. Negishi, S. Endo, H. Matsui, and N. Toyota, Synth. Met. **135-136**, 565 (2003).
[25] N. Toyota, Y. Abe, T. Kuwabara, E. Negishi, and H. Matsui, J. Phys. Soc. Jpn. (to be published).
[26] Y. Tokura, H. Okamoto, T. Koda, T. Mitani, and G. Saito, Phys. Rev. B **38**, 2215 (1988).
[27] Y. Iwasa, T. Koda, S. Koshihara, Y. Tokura, N. Iwasawa, and G. Saito, Phys. Rev. B **39**, 10 441 (1989).
[28] H. Matsui, H. Tsuchiya, E. Negishi, H. Uozaki, Y. Ishizaki, Y. Abe, S. Endo, and N. Toyota, J. Phys. Soc. Jpn. **70**, 2501 (2001).
[29] H. Matsui, H. Tsuchiya, and N. Toyota, J. Phys. Soc. Jpn. **71**, 668 (2002).
[30] O. Klein, S. Donovan, M. Dressel, and G. Grüner, Int. J. Infrared Millim. Waves **14**, 2423 (1993).
[31] C. P. Poole, *Electron Spin Resonance* (Dover, New York, 1996).
[32] L.I. Buranov and I.F. Shchegolev, Instrum. Exp. Tech. **14**, 528 (1971).
[33] H. Ito, M.V. Kartsovnik, H. Ishimoto, K. Kono, H. Mori, N.D. Kushch, G. Saito, T. Ishiguro, and S. Tanaka, Synth. Met. **70**, 899 (1995).
[34] V.N. Laukhin, A. Audouard, H. Rakoto, J.M. Broto, F. Goze, G.

Coffe, L. Brossard, J.P. Redoules, M.V. Kartsovnik, N.D. Kushch, L.I. Buravov, A.G. Khomenko, E.B. Yagubskii, S. Askenazy, and P. Pari, Physica B **211**, 282 (1995).
[35] T. Sasaki, N. Yoneyama, A. Matsuyama, and N. Kobayashi, Phys. Rev. B **65**, 060505 (2002).
[36] S. Donovan, Y. Kim, L. Degiorgi, M. Dressel, G. Grüner, and W. Wonneberger, Phys. Rev. B **49**, 3363 (1994).
[37] J.L. Musfeldt, M. Poirier, P. Batail, and C. Lenoir, Phys. Rev. B **51**, 8347 (1995).
[38] Y. Takano, K. Hiraki, H. Yamamoto, T. Nakamura, and T. Takahashi, J. Phys. Chem. Solids **62**, 393 (2001).
[39] M. Dressel, G. Grüner, J.P. Pouget, A. Breining, and D. Schweitzer, J. Phys. I **4**, 579 (1994).
[40] Y. Abe, H. Uozaki, H. Tsuchiya, E. Negishi, Y. Ishizaki, H. Matsui, S. Endo, and N. Toyota, Synth. Met. **133-134**, 563 (2003).
[41] C. Hotta and H. Fukuyama, J. Phys. Soc. Jpn. **69**, 2577 (2000).
[42] H. Uozaki *et al.* (unpublished).
[43] T. Suzuki, H. Matsui, H. Tsuchiya, E. Negishi, K. Koyama, and N. Toyota, Synth. Met. **135-136**, 567 (2003).
[44] T. Suzuki, H. Matsui, H. Tsuchiya, E. Negishi, K. Koyama, and N. Toyota, Phys. Rev. B **67**, 020408 (2003).
[45] J.I. Oh, M.J. Naughton, T. Courcet, I. Malfant, P. Cassoux, M. Tokumoto, H. Akutsu, H. Kobayashi, and A. Kobayashi, Synth. Met. **103**, 1861 (1999).
[46] T. Sasaki, H. Uozaki, S. Endo, and N. Toyota, Synth. Met. **120**, 759 (2001).
[47] M. Watanabe, S. Komiyama, R. Kiyanagi, Y. Noda, E. Negishi, and N. Toyota, J. Phys. Soc. Jpn. **72**, 452 (2003).
[48] E. Negishi, H. Uozaki, Y. Ishizaki, H. Tsuchiya, S. Endo, Y. Abe, H. Matsui, and N. Toyota, Synth. Met. **133-134**, 555 (2003).
[49] S. Endo, T. Goto, T. Fukase, H. Matsui, H. Uozaki, H. Tsuchiya, E. Negishi, Y. Ishizaki, Y. Abe, and N. Toyota, J. Phys. Soc. Jpn. **71**, 732 (2002).
[50] S. Endo, T. Goto, T. Fukase, H. Matsui, H. Uozaki, H. Tsuchiya, E. Negishi, Y. Ishizaki, Y. Abe, and N. Toyota, Synth. Met. **133-134**, 557 (2003).
[51] D.S. Chow, F. Zamborszky, B. Alavi, D.J. Tantillo, A. Baur, C.A. Merlic, and S.E. Brown, Phys. Rev. Lett. **85**, 1698 (2000).
[52] P. Monceau, F. Nad, and S. Brazovskii, Phys. Rev. Lett. **86**, 4080 (2001).
[53] H. Kobayashi (private communication).
[54] N. W. Ashcroft and N. D. Mermin, *Solid State Physics* (Saunders College, Fort Worth, TX, 1976).
[55] M.A. Ruderman and C. Kittel, Phys. Rev. **96**, 99 (1954); T. Kasuya, Prog. Theor. Phys. **16**, 45 (1956); K. Yoshida, Phys. Rev. **106**, 893 (1957).
[56] L. Degiorgi, Rev. Mod. Phys. **71**, 687 (1999).
[57] A.M. Awasthi, L. Degiorgi, G. Grüner, Y. Dalichaouch, and M.B. Maple, Phys. Rev. B **48**, 10 692 (1993).
[58] P. Tran, S. Donovan, and G. Grüner, Phys. Rev. B **65**, 205102 (2002).
[59] T. Shibauchi, N. Katase, T. Tamegai, K. Uchonokura, T. Takabatake, G. Nakamoto, and A.A. Menovsky, Phys. Rev. B **56**, 8277 (1997).
[60] K.A. Müller and H. Burkard, Phys. Rev. **19**, 3593 (1979).
[61] L.E. Cross, Ferroelectrics **76**, 241 (1987).
[62] G.A. Smolenskii, V.A. Isupov, A.I. Agranovskaya, and S.N. Popov, Fiz. Tverd. Tela (Leningrad) **2**, 2906 (1960) [Sov. Phys. Solid State **2**, 2584 (1961)].
[63] S. Horiuchi, R. Kumai, Y. Okimoto, and Y. Tokura, Phys. Rev. Lett. **85**, 5210 (2000).
[64] Q.M. Zhang, V. Bharti, and X. Zhao, Science **280**, 2101 (1998).
[65] M. Watanabe and Y. Noda (private communication).